Transport properties in a multi-terminal regular polygonal quantum ring with Rashba spin–orbit coupling*

Tang Han-Zhao(唐翰昭)[a], Zhai Li-Xue(翟利学)[a], and Liu Jian-Jun(刘建军)[a)b)†]

[a] *Department of Physics and Hebei Advanced Thin Film Laboratory, Hebei Normal University, Shijiazhuang* 050024, *China*
[b] *Department of Physics, Shijiazhuang University, Shijiazhuang* 050035, *China*

(Received 1 April 2012; revised manuscript received 18 June 2012)

Transport properties in a multi-terminal regular polygonal quantum ring with Rashba spin–orbit coupling (SOC) are investigated analytically using quantum networks and the transport matrix method. The results show that conductances remain at exactly the same values when the output leads are located at axisymmetric positions. However, for the nonaxisymmetrical case, there is a phase difference between the upper and lower arm, which leads to zero conductances appearing periodically. An isotropy of the conductance is destroyed by the Rashba SOC effect in the axisymmetric case. In addition, the position of zero conductance is regulated with the strength of the Rashba SOC.

Keywords: multi-terminal quantum ring, Rashba spin–orbit coupling, transport property

PACS: 03.65.Nk, 05.60.Gg, 71.70.Ej **DOI:** 10.1088/1674-1056/21/12/120303

1. Introduction

The manipulation of electron spin in a low-dimensional semiconductor structure has attracted considerable attention in recent decades.[1] The generation of spin-polarized current and its appropriate manipulation in a controllable environment, especially in a semiconductor system, have led to many significant theoretical and experimental results.[2−4] Suitable means for controlling electron spin on the mesoscopic scale are provided by the quantum interference effects in coherent ring conductors under the influence of electromagnetic potentials, such as the Aharonov–Bohm (AB) effect[5] and the Aharonov–Casher (AC) effect.[6] The transport properties of mesoscopic AB and AC rings coupled to current leads have been extensively studied in various aspects such as AB flux, precession and interference effects.[7−15] In particular, transport through quantum rings containing several confined electrons has been realized within the last decade.[16,17] Recently, quantum rings with multiple arms have been studied.[18−30]

As a relativistic effect, the Rashba spin–orbit coupling (SOC) effect has also been extensively studied. The Rashba SOC in quantum rings may lead to an electron localization phenomenon. While the properties of an electric current are not related to how a wire is bent, SOC apparently depends on the speed and direction of electronic movement, which may be affected by the extent to which a wire is bent. Therefore, the electron transport properties in multi-terminal regular polygonal quantum rings, which are subjected to the Rashba SOC, will be greatly changed by the Rashba effect. Besides circular quantum ring models,[18−20] other geometrical ring shapes have also been investigated.[21−29] Bercioux *et al.*[22] have discussed a quantum network extending in one dimension, which is a chain of square loops connected at one vertex. Koga *et al.*[26] and van Veenhuizen *et al.*,[27] who proposed a ballistic spin interferometer using square loop geometry, investigated the spin–orbit induced spin interference patterns of ballistic electrons traveling along any regular polygon. Szafran and Poniedzialek[30] studied the electron transport probability through a semiconductor quantum ring with one input and two output terminals when an elastic scattering site was present.

Research on the spin transport characteristics of regular polygonal quantum rings is a quantum network problem. By creating the electronic quantum wave functions for a complex network, and by cal-

*Project supported by the National Natural Science Foundation of China (Grant No. 61176089) and Hebei Provincial Natural Science Foundation, China (Grant No. A2011205092).

†Corresponding author. E-mail: liujj@mail.hebtu.edu.cn

© 2012 Chinese Physical Society and IOP Publishing Ltd

culating their simultaneous equations, we can obtain analytic solutions of the transport properties for any quantum network. Based on previous work, quantum transport of electrons through two terminals in arbitrary equilateral polygonal quantum rings with Rashba SOC was studied.[21,29,31] To the best of our knowledge, the effect of Rashba SOC on electron transport in multi-terminal regular polygonal quantum rings has not been investigated thoroughly. However, experimental studies[32] for multi-terminal quantum rings with magnetic fields have been reported. Therefore, we are interested in building a theoretical model for the transport property of a regular polygonal quantum ring with Rashba SOC where there are one input and two alterable output terminals.

In this paper, we analytically solve, by using a typical quantum network method, the scattering problem of transporting electrons through a multi-terminal equilateral polygonal quantum ring. By means of the Landauer–Büttiker formula, we also obtain the conductance of the electrons. In this study, we find a difference in conductance between the output terminals for the axisymmetric and nonaxisymmetric cases.

The rest of the present paper is organized as follows. In Section 2, we provide a theoretical model to calculate the conductance for a polygonal quantum ring. Numerical results and discussion of the transport properties are described in Section 3. Finally, we present our conclusions in Section 4.

2. Model and formulas

We consider a regular polygon with $3N$ vertices coupled to three terminals as shown in Fig. 1. The polygon is coupled to three one-dimensional (1D) leads which are free of SOC. The two output leads are located at symmetric or asymmetric positions with respect to the input lead. We assume that the width of the structure is narrow enough compared with the length of the structure so that the energy spacing between the quantum energy levels, produced by the transverse confinement, is much larger than the energy range of the longitudinal transport.

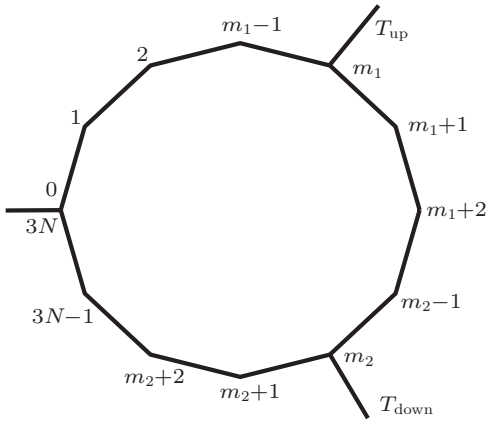


Fig. 1. A 1D polygonal quantum ring coupled to one input and two output terminals. Vertices are connected by single-channel ballistic quantum wires with Rashba SOC. $T_{\rm up}$ and $T_{\rm down}$ represent transmission coefficients of the upper and lower arms, respectively.

We simplify the structure into a 1D equation with the coordinate axis along the longitudinal direction of the structure.[33] Neglecting subband hybridization,[34,35] the Hamiltonian for a single-channel wire along a generic direction $\hat{\gamma}$ in the x–y plane is[2]

$$\hat{H} = \frac{p_\gamma^2}{2m^*} - \frac{\hbar k_{\rm so}}{m^*} p_\gamma (\hat{\sigma} \times \hat{z}) \cdot \hat{\gamma}, \tag{1}$$

where $p_\gamma = -\mathrm{i}\hbar\partial/\partial l$ is the momentum operator in the $\hat{\gamma}$ direction, m^* is the effective mass of the electron, and $\hat{\sigma}$ is the vector of the Pauli matrices. The SOC strength $k_{\rm so}$ is related to the spin precession length $L_{\rm so}$ by $L_{\rm so} = \pi/k_{\rm so}$. When an electron with energy of E is injected from the left wire into a regular polygon as shown in Fig. 1, the wave functions on the external leads are

$$\begin{aligned} &\psi_0 = A\,\mathrm{e}^{\mathrm{i}k_0 l} + B\,\mathrm{e}^{-\mathrm{i}k_0 l}, \quad \psi_{m_1} = F\,\mathrm{e}^{\mathrm{i}k_0 l}, \\ &\psi_{m_2} = C\,\mathrm{e}^{\mathrm{i}k_0 l}, \end{aligned} \tag{2}$$

where l is the length of the semi-infinite input/output lead with the origin fixed at the position of the input/output node; k_0 is the wave-vector corresponding to $k_0 = \sqrt{2m^*E}/\hbar$; A and B are the injection and reflection coefficients; F and C are the upper and lower arms transmission coefficients, respectively. In order to investigate the transport properties of the network, the wave function for a bond (quantum wire) connecting the nodes α and β along the direction $\hat{\gamma}_{\alpha\beta}$ is[22]

$$\begin{aligned} \Psi_{\alpha\beta}(l) = {} & \frac{\mathrm{e}^{\mathrm{i}k_{\rm so} l(\hat{\sigma}\times\hat{z})\cdot\hat{\gamma}_{\alpha\beta}}}{\sin(kl_{\alpha\beta})} \{\sin[k(l_{\alpha\beta}-l)]\Psi_\alpha \\ & + \sin(kl)\,\mathrm{e}^{-\mathrm{i}k_{\rm so} l_{\alpha\beta}(\hat{\sigma}\times\hat{z})\cdot\hat{\gamma}_{\alpha\beta}}\Psi_\beta\}, \end{aligned} \tag{3}$$

where $k = \sqrt{k_0^2 + k_{\rm so}^2}$; r is the coordinate along the bond whose length is $l_{\alpha\beta}$; spinors Ψ_α and Ψ_β are the values of the wave function at nodes α and β; $\hat{\gamma}$ is the position of the electron in the quantum wire. At vertices α and β, $\gamma_\alpha = 0$ and $\gamma_\beta = l_{\alpha\beta}$. The spin precession due to the Rashba effect is described by the exponentials that contain Pauli matrices in Eq. (3), which is the key step in order to generalize the existing method of studying quantum networks[36,37] in

the presence of Rashba SOC. The wave function of the whole network is obtained by using Griffith's boundary conditions[12,38]

$$\sum_{\langle\alpha,\beta\rangle}\frac{\partial}{\partial l}[\,\mathrm{e}^{-\mathrm{i}k_{\mathrm{so}}r(\hat{\sigma}\times\hat{z})\cdot\hat{\gamma}_{\alpha\beta}}]\Psi_{\alpha\beta}=0. \tag{4}$$

Here, the sum $\sum_{\langle\alpha,\beta\rangle}$ runs over all nodes β that are connected by a single bond to the node α. For internal nodes, the conditions for continuity of the probability current for a generic node α, Eq. (4) simplifies into $M_{\alpha\alpha}\psi_\alpha - M_{\alpha\beta}\psi_\beta = 0$, where $M_{\alpha\alpha} = \sum_{\langle\alpha,\beta\rangle}\cot(kl_{\alpha\beta})$, $M_{\alpha\beta} = R_{\alpha\beta}/\sin(kl_{\alpha\beta})$, and $R_{\alpha\beta} = \mathrm{e}^{-\mathrm{i}k_{\mathrm{so}}r(\hat{\sigma}\times\hat{z})\cdot\hat{\gamma}_{\alpha\beta}}$. For external nodes, the conditions become

$$2\cos(kl)\psi_a - \sum_{\langle a,b\rangle}R_{ab}\psi_b = 0, \tag{5}$$

$$2\cos(kl)\psi_0 - \sum_{\langle 0,b\rangle}R_{0b}\psi_b = \frac{\mathrm{i}k_0\sin(kl)}{k}(B-A), \tag{6}$$

$$2\cos(kl)\psi_{m_1} - \sum_{\langle m_1,b\rangle}R_{m_1b}\psi_b = \frac{\mathrm{i}k_0\sin(kl)}{k}F, \tag{7}$$

$$2\cos(kl)\psi_{m_2} - \sum_{\langle m_2,b\rangle}R_{m_2b}\psi_b = \frac{\mathrm{i}k_0\sin(kl)}{k}C. \tag{8}$$

The reflection and transmission coefficients can be obtained by solving the linear system of equations arising from the Griffith's boundary conditions, which are related to Eqs. (5)–(8). The amplitude A can be modulated experimentally. To solve these equations, we evaluate Eq. (5) for independent clockwise ($\psi^{(+)}$) and counter-clockwise ($\psi^{(-)}$) traveling wave functions

$$\begin{aligned}\psi_n^{(+)} &= \mathrm{e}^{\mathrm{i}kl}\psi_0 - R_{n,n-1}\psi_{n-1},\\ \psi_n^{(-)} &= \mathrm{e}^{-\mathrm{i}kl}\psi_0 - R_{n,n-1}\psi_{n-1},\end{aligned} \tag{9}$$

where the length of a polygonal ring segment is $l_{\alpha\beta}\equiv l$, and $L = Nl$. Since there are $3N$ vertices in the ring, there are $3N+3$ functions, each of which contains a subset of ψ_0, ψ_1, …, ψ_{3N}, B, C, and F. For convenience, we define three parameters ρ_1, ρ_2, and ξ, as $\rho_1{=}m_1/3N$, $\rho_2{=}m_2/3N$, and $\xi = 3kL$. Finally we obtain

$$\frac{-\sin[(1+\rho_1-\rho_2)kL](A+B)+\sin[(1-\rho_2)\xi]W_{0,m_1}F+\sin(\rho_1\xi)D_{3N,m_2}C}{\sin(\rho_1\xi)\sin[(1-\rho_2)\xi]} = -\mathrm{i}\frac{k_0}{k}(B-A), \tag{10}$$

$$\frac{-\sin(\rho_2\xi)F+\sin(\rho_1\xi)U_{m_1,m_2}C+\sin[(\rho_2-\rho_1)\xi]W_{m_1,0}(A+B)}{\sin(\rho_1\xi)\sin[(\rho_2-\rho_1)\xi]} = -\mathrm{i}\frac{k_0}{k}F, \tag{11}$$

$$\frac{-\sin[(1-\rho_1)\xi]C+\sin[(1-\rho_2)\xi]U_{m_2,m_1}F+\sin[(\rho_2-\rho_1)\xi]D_{m_2,3N}(A+B)}{\sin[(1-\rho_2)\xi]\sin[(\rho_2-\rho_1)\xi]} = -\mathrm{i}\frac{k_0}{k}C, \tag{12}$$

where $W_{m_1,0} = R_{m_1,m_1-1}R_{m_1-1,m_1-2},\ldots,R_{1,0}$, $U_{m_2,m_1} = R_{m_2,m_2-1}R_{m_2-1,m_2-2},\ldots,R_{m_1+1,m_1}$, $D_{3N,m_2} = R_{3N,3N-1}R_{3N-1,3N-2},\ldots,R_{m_2+1,m_2}$, and $W_{m_1,0} = W_{0,m_1}^{-1}$, $U_{m_2,m_1} = U_{m_1,m_2}^{-1}$, $D_{3N,m_2} = D_{m_2,3N}^{-1}$.

Since $R_{\alpha\beta} = \mathrm{e}^{[-\mathrm{i}k_{\mathrm{so}}l_{\alpha\beta}(\hat{z}\times\hat{\gamma}_{\alpha\beta})\cdot\boldsymbol{\sigma}]}$, the above equations for $W_{m_1,0}$, U_{m_2,m_1}, and D_{3N,m_2} can be rewritten as

$$\begin{aligned}W_{m_1,0} &= \cos(m_1\phi)[\cos(\rho_1\pi)+\mathrm{i}\sin(\rho_1\pi)\sigma_z] - \mathrm{i}\frac{\sin(m_1\phi)}{\sin\phi}\sin\alpha\left[\sin\left(\frac{2\rho_1-3}{2}\pi\right)\sigma_x+\cos\left(\frac{2\rho_1-3}{2}\pi\right)\sigma_y\right]\\ &\quad+\mathrm{i}\frac{\sin(m_1\phi)}{\sin\phi}\cos\alpha\sin\frac{\delta}{2}[\sin(\rho_1\pi)-\mathrm{i}\cos(\rho_1\pi)\sigma_z],\end{aligned} \tag{13}$$

$$\begin{aligned}U_{m_2,m_1} &= \cos[(m_2-m_1)\phi]\{\cos[(\rho_2-\rho_1)\pi]+\mathrm{i}\sin[(\rho_2-\rho_1)\pi]\sigma_z\}\\ &\quad-\mathrm{i}\frac{\sin[(m_2-m_1)\phi]}{\sin\phi}\sin\alpha\left[\sin\left(\frac{3-2\rho_1-2\rho_2}{2}\pi\right)\sigma_x+\cos\left(\frac{3-2\rho_1-2\rho_2}{2}\pi\right)\sigma_y\right]\\ &\quad+\mathrm{i}\frac{\sin[(m_2-m_1)\phi]}{\sin\phi}\cos\alpha\sin\frac{\delta}{2}\{\sin[(\rho_2-\rho_1)\pi]-\mathrm{i}\cos[(\rho_2-\rho_1)\pi]\sigma_z\},\end{aligned} \tag{14}$$

$$\begin{aligned}D_{3N,m_2} &= \cos[(3N-m_2)\phi]\{\cos[(1-\rho_2)\pi]+\mathrm{i}\sin[(1-\rho_2)\pi]\sigma_z\}\\ &\quad-\mathrm{i}\frac{\sin[(3N-m_2)\phi]}{\sin\phi}\sin\alpha\left[\sin\left(\frac{2\rho_2-1}{2}\pi\right)\sigma_x+\cos\left(\frac{2\rho_2-1}{2}\pi\right)\sigma_y\right]\\ &\quad+\mathrm{i}\frac{\sin[(3N-m_2)\phi]}{\sin\phi}\cos\alpha\sin\frac{\delta}{2}\{\sin[(1-\rho_2)\pi]-\mathrm{i}\cos[(1-\rho_2)\pi]\sigma_z\}.\end{aligned} \tag{15}$$

Moreover, we can obtain the transmission coefficients to be

$$F = \frac{2\mathrm{i}\frac{k_0}{k}d[cW_{m_1,0}-\sin(\rho_1\xi)U_{m_1,m_2}D_{m_2,3N}]}{a\{\sin[(1-\rho_2)\xi]\sin(\rho_1\xi)-bc\}+\sin[(\rho_2-\rho_1)\xi]\{c\sin[(1-\rho_2)\xi]+b\sin(\rho_1\xi)\}-d(e+e^*)}A, \tag{16}$$

$$C = \frac{2\mathrm{i}\dfrac{k_0}{k} d\{bD_{m_2,3N} - \sin[(1-\rho_2)\xi]U_{m_2,m_1}W_{m_1,0}\}}{a\{\sin[(1-\rho_2)\xi]\sin(\rho_1\xi) - bc\} + \sin[(\rho_2-\rho_1)\xi]\{c\sin[(1-\rho_2)\xi] + b\sin(\rho_1\xi)\} - d(e+e^*)} A, \quad (17)$$

where

$$a = \mathrm{i}\frac{k_0}{k}\sin(\rho_1\xi)\sin[(1-\rho_2)\xi] - \sin[(1+\rho_1-\rho_2)\xi],$$
$$b = \mathrm{i}\frac{k_0}{k}\sin(\rho_1\xi)\sin[(\rho_2-\rho_1)\xi] - \sin(\rho_2\xi),$$
$$c = \mathrm{i}\frac{k_0}{k}\sin[(1-\rho_2)\xi]\sin[(\rho_2-\rho_1)\xi] - \sin[(1-\rho_1)\xi],$$
$$d = \sin[(1-\rho_2)\xi]\sin[(\rho_2-\rho_1)\xi]\sin(\rho_1\xi),$$
$$e = W_{0,m_1}U_{m_1,m_2}D_{m_2,3N}.$$

The conductance in the mesoscopic structure under consideration can be derived by the Landauer–Büttiker conductance formula,[38,39] which in our case is

$$G = \frac{e^2}{h}\sum_{\langle\sigma=\uparrow,\downarrow\rangle}|T_\sigma|^2 = G_\uparrow + G_\downarrow. \quad (18)$$

3. Results and analysis

3.1. Axisymmetric case

In the axisymmetric case, when the output leads are located at a symmetric position with respect to the input lead, for example, when $m_1 = N$ and $m_2 = 2N$,

$$T = \frac{4\dfrac{k_0^2}{k^2}\sin^2(kL)\left\{\dfrac{k_0^2}{k^2}\sin^2(kL) + 4\cos^2(kL) + 1 + [2\cos(kL) + \mathrm{i}\dfrac{k_0}{k}\sin(kL)](e+e^*)\right\}}{T_1^2 + T_2^2}, \quad (19)$$

where

$$T_1 = -e - e^* - 3\frac{k_0^2}{k^2}\sin^2(kL) + 12\cos^2(kL) - 6\frac{k_0^2}{k^2}\sin^2(kL)\cos(kL) + 8\cos^3(kL),$$
$$T_2 = 12\frac{k_0}{k}\sin(kL)\cos(kL) + \frac{k_0^3}{k^3}\sin^3(kL) - 12\frac{k_0}{k}\sin(kL)\cos^2(kL).$$

In the absence of SOC ($k_{\mathrm{so}} = 0$),

$$T = \frac{4\sin^2(k_0L)[\sin^2(k_0L) + 4\cos^2(k_0L) + 1 + 4\cos(k_0L)]}{[-3\sin^2(k_0L) + 12\cos^2(k_0L) - 6\sin^2(k_0L)\cos(kL) + 8\cos^3(k_0L)]^2 + [12\sin(k_0L)\cos(k_0L) + \sin^3(k_0L) - 12\sin(k_0L)\cos^2(k_0L)]^2}. \quad (20)$$

From Eq. (20), we can see that the systematic transmission coefficient T depends only on the dynamic phase k_0l from the input node to the output node of the nanostructure for the axisymmetric case in the absence of Rashba SOC. Therefore, neither the shape nor the segment length, l, of a regular polygonal quantum ring influences the electronic quantum transport properties when the length between the input and the output leads, Nl, is kept constant. In addition, from Eq. (20), we can see that the spin state of an incident electron is invariant in the transport process. Electronic quantum transport is not related to an electron's spin degree of freedom in normal metal wires, which is an outstanding feature of traditional electronics.

The conductance as a function of k_0L/π in the absence of Rashba SOC for an axisymmetric system is displayed in Fig. 2. Because the conductance is periodic, only one period is shown here. The curves in the figure, which are characterized by a set of zeros and poles, show a peculiar resonant behaviour. Zero conductances appear at $k_0L = m\pi$, where m is an integer. The zero conductances correspond to eigenstates in a closed ring. The electrons entering into the ring will spend more time in the ring before being reflected or transmitted because there is coupling between the ring and the leads. Electrons that spend a long time in the closed ring must be in an eigenstate of the closed ring. There are two key elements that lead to the oscillation of the conductance for symmetric configurations. The first is due to imperfect transmission caused by coupling between the ring and the leads which results in resonance as a consequence of backscattering effects.[7] The second is quantum interference between the alternate paths, clockwise, and counter-clockwise. Since this is an axisymmetric system, the phase of the electrons transmitted in the upper arm is the same as that in the lower arm. The conductances have exactly

the same values when the output leads are located at axisymmetric positions, which are consistent with the results for a circular quantum ring given by Wang and Chang[15] and by Szafran and Poniedzialek.[30] An isotropy in the conductance is induced by the symmetric positions of the output leads. $T_{\rm up}$ and $T_{\rm down}$ can be found from Eqs. (16) and (17). They each make the same contributions to the total transmission coefficient. The conductance of one output terminal varies from 0 to $0.42G/G_0$. A similar model for the transport properties of a tri-terminal ring with equal arms has been proposed and obtained by Szafran and Poniedzialek,[30] who found that the transmission coefficient varies from 0 to 0.42 at any output terminal in the absence of a magnetic field. One can notice that the variation range of the conductance that we calculated is consistent with this phenomenon.

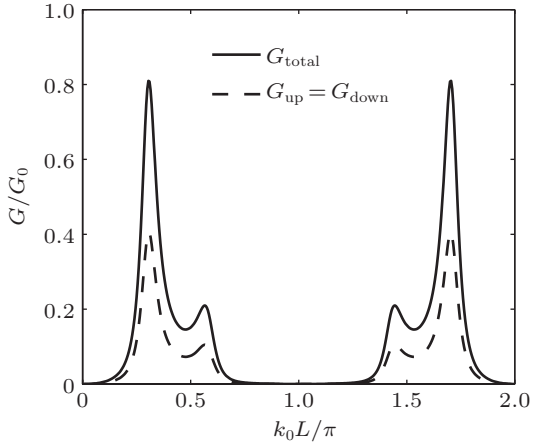


Fig. 2. Conductances of a regular hexagonal quantum ring versus k_0L/π for $k_{\rm so}=0$ in an axisymmetric case with ρ_1=1/3 and ρ_2=2/3. $G_{\rm total}$, $G_{\rm up}$, and $G_{\rm down}$ represent the total conductance and conductances of the upper and lower arms, respectively.

As the number of vertices increases, the equilateral polygon turns into a circular ring. From our calculations for polygonal quantum rings, the conductance pattern is invariant with N increasing. Therefore, we can infer that the conductance remains constant as the number of the vertices increases; the conductance is independent of the number of vertices in the absence of Rashba SOC for the axisymmetric case. The transport properties of a circular ring can be extrapolated from our results.

3.2. Nonaxisymmetric case

The results from Eq. (19) for the total conductance in a nonaxisymmetric system in the absence of Rashba SOC are shown in Fig. 3(a). It is interesting to note that the total conductance of the quantum ring varies as the location of output terminals changes. Due to the alteration of the output leads, the electronic phase changes in the nonaxisymmetric system. Because the electronic wave functions for the upper and lower arms are different, new locations for zero and pole conductances appear. What should be noted in Fig. 3(a) is that the transport property changes dramatically when $m=k_0L/\pi$ is an integer. In the nonaxisymmetric case, the change in the position between the two output arms can cause a phase difference that leads to destructive interference at the lead positions and may result in zeros for the transmission.[40] In Fig. 3(b), the conductances for both the upper and lower arms in the nonaxisymmetric system are displayed. It is obvious that $G_{\rm up}$ is different from $G_{\rm down}$ in this nonaxisymmetric example. The conductance at a terminal will change if the location of the other terminal is adjusted. In the absence of Rashba SOC,

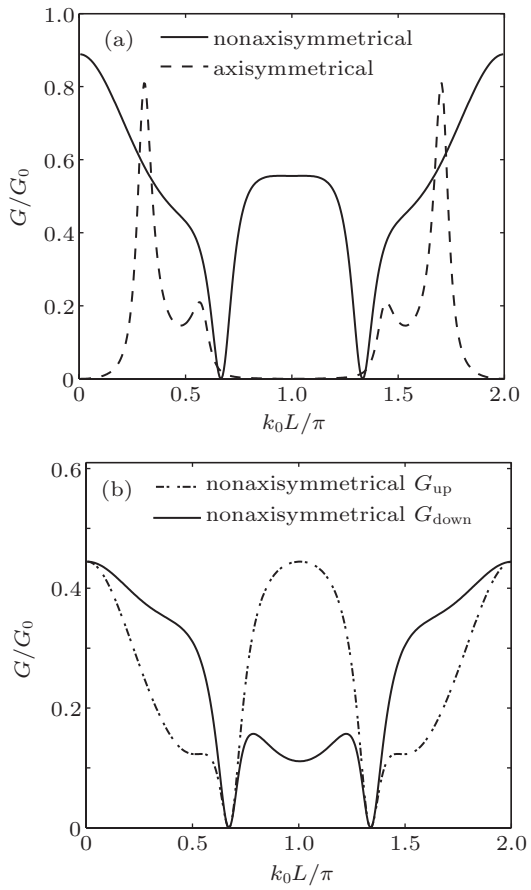


Fig. 3. (a) Total conductances of a regular hexagonal quantum ring versus k_0L/π in the absence of Rashba SOC for axisymmetric (ρ_1=1/3 and ρ_2=2/3) and nonaxisymmetric systems (ρ_1=1/6 and ρ_2=2/3). (b) Conductances of an output terminal versus k_0L/π in the absence of Rashba SOC for a nonaxisymmetric system (ρ_1=1/6 and ρ_2=2/3).

the conductance of a polygonal quantum ring depends mainly on the phase of the electron wave function and the phase difference between the upper and the lower arm. For a given $L = Nl$ system, the phase of the electron wave function is controlled mainly by the energy of the incident electron. If the input terminal location is fixed, the phase difference can be conveniently modified when the position of the output terminal is adjusted. When the position of one output terminal varies, the clockwise and counterclockwise electron wave functions, and therefore the transport properties, also change in the other output terminal. Therefore, we can control the transport property of one output terminal by changing the location of the other output terminal.

3.3. Finite Rashba SOC ($k_{\rm so} \neq 0$)

The effect of the Rashba SOC on the transport probability through the axisymmetric polygonal ring is illustrated in Fig. 4(a). We notice that the external Rashba SOC introduces an asymmetry for the conductance between the upper and lower output terminals. For arbitrary two-terminal equilateral polygonal rings, an oscillation can be induced by the finite Rashba SOC effect.[29,31] For equilateral polygonal quantum rings with three terminals, it is demonstrated that the Rashba SOC not only produces an oscillation in the amplitude but also introduces a distinct imbalance between the electron-transport probabilities of the two output leads, as it shows in Fig. 4(a). The Rashba SOC behaves like an effective in-plane momentum-dependent magnetic field that induces a phase difference between the electrons traveling clockwise and those traveling counterclockwise along the ring's upper and lower arms. The phase induced by Rashba SOC depends on the path of the electron. By comparing Fig. 2 with Fig. 4(a), we can draw a conclusion that the isotropy in the conductance is destroyed by the Rashba SOC effect in the axisymmetric case. Thus, the conductance displays asymmetric features for the axisymmetric positions of the output leads.

The conductance for a nonaxisymmetric system with finite Rashba SOC is displayed in Fig. 4(b). We take a regular hexagon ($N = 2$) as an example. We use an experimentally allowed strength for the Rashba SOC, similar to that used by Koga *et al.*[28] The curves in Fig. 4(b) show that the conductances in the presence of Rashba SOC vary periodically with a period of 2π. We can see from Fig. 4(b) that the Rashba SOC effect lifts the conductance zeros. The conductance pattern of a 1D ring in the presence of Rashba SOC oscillates periodically and transforms when we change the strength of the Rashba SOC. In a quasi-1D system, the real conductance zeros appear under the condition of conserved time reversal symmetry (TRS).[41] In the quasi-1D AB ring, the application of an external magnetic field modifies the conductance zeros-pole structure, shifting the transmission zeros away from the real axis.[42] Therefore, the lifted zeros are related to the breaking of TRS. Similar to breaking TRS in an AB ring, lifting the real conductance zeros in an AC ring can be related to breaking spin–parity symmetry. In the asymmetric system, the asymmetrically coupled leads break the spin–parity symmetry,

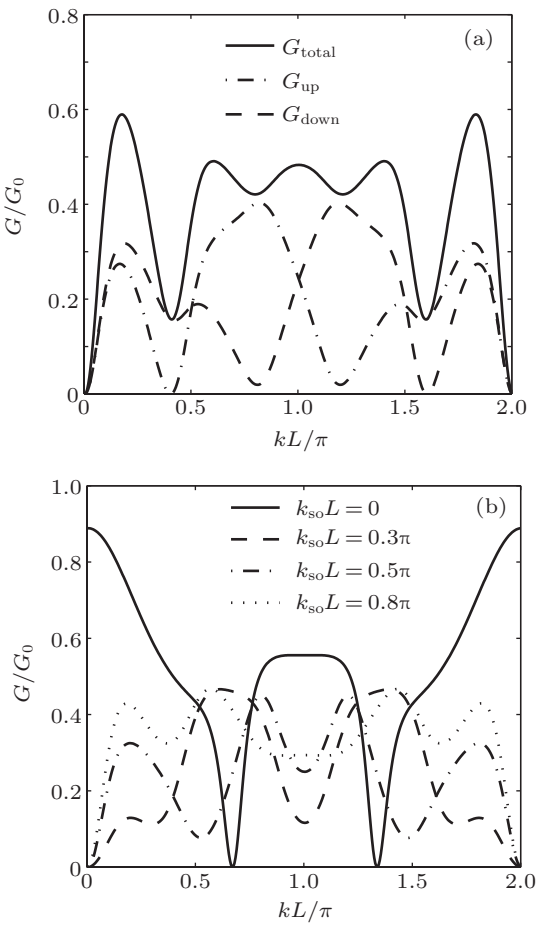


Fig. 4. (a) Conductances for the output terminals and total conductance versus kL for the axisymmetric system (ρ_1=1/6 and ρ_2= 5/6) when $k_{\rm so}$=0.3π. (b) Total conductances versus kL for the nonaxisymmetric system (ρ_1=1/6 and ρ_2=2/3) when $k_{\rm so}$= 0, 0.3π, 0.5π, and 0.8π.

shifting the transmission zeros away from the real axis. In the presence of finite Rashba SOC, the conductance zeros correspond to a frequency of precession that reproduces the incident spin orientation at the output terminal.

By using a regular polygonal quantum ring with alterable output terminals, we propose a multi-terminal ballistic interferometer. For the axisymmetric and nonaxisymmetric cases, we can control the conductance at the terminal by varying the strength of Rashba SOC. Our model provides a method of controlling the conductance of a polygonal quantum ring that could potentially be used in some type of interferometers. We would like to stress that the observation of our predicted conductance patterns for polygonal quantum rings is within the reach of today's technology, for example, in experiments of semiconductor heterostructures with a two-dimensional electron gas (2DEG), e.g., an InGaAs-based 2DEG, which has an internal electric field due to an asymmetric quantum well which can produce asymmetric quantum rings. It is very encouraging to see that our model provides a new theoretical prediction and sheds some light on this field.

4. Conclusions

In this paper, we studied the transport properties of a 1D regular polygonal quantum ring with multiple terminals where the ring is subjected to Rashba SOC. By using a typical quantum network method, we analytically solved the scattering problem and found relevant formulas for transmission probabilities. Our theoretical results show that the conductances for each of the output terminals have exactly the same values when they are located at axisymmetric positions. However, for the nonaxisymmetric case, there is a phase difference between the upper and lower arms, which leads to zero conductances appearing periodically. We can also control the transport property of one output terminal by changing the location of the other output terminal. The positions of the zero conductances can be regulated by Rashba SOC. In addition, the anisotropy of the conductance is induced by the Rashba SOC effect in the axisymmetric case. Furthermore, the anisotropy of the spin transport should play an important role in the potential application for electrical spintronic devices.

References

[1] Prinz G A 1998 *Science* **282** 1660

[2] Bychkov Y A and Rashba E I 1984 *J. Phys.* C **17** 6039

[3] Timp G, Chang A M, Cunningham J E, Chang T Y, Mankiewich P, Behringer R and Howard R E 1987 *Phys. Rev. Lett.* **58** 2814

[4] Nitta J, Akazaki T, Takayanagi H and Enoki T 1997 *Phys. Rev. Lett.* **78** 1335

[5] Aharonov Y and Bohm D 1959 *Phys. Rev.* **115** 485

[6] Aharonov Y and Casher A 1984 *Phys. Rev. Lett.* **53** 319

[7] Büttiker M, Imry Y and Azbel M Y 1984 *Phys. Rev.* A **30** 1982

[8] Loss D, Goldbart P and Balatsky A V 1990 *Phys. Rev. Lett.* **65** 1655

[9] Aronov A G and Lyanda-Geller Y B 1993 *Phys. Rev. Lett.* **70** 343

[10] Frustaglia D, Hentschel M and Richter K 2004 *Phys. Rev.* B **69** 155327

[11] Molnár B, Peeters F M and Vasilopoulos P 2004 *Phys. Rev.* B **69** 155335

[12] Frustaglia D and Richter K 2004 *Phys. Rev.* B **69** 235310

[13] Aeberhard U, Wakabayashi K and Sigrist M 2005 *Phys. Rev.* B **72** 075328

[14] Citro R, Romeo F and Marinaro M 2006 *Phys. Rev.* B **74** 115329

[15] Wang M and Chang K 2008 *Phys. Rev.* B **77** 125330

[16] Fuhrer A, Lüscher S, Ihn T, Heinzel T, Ensslin K, Wegscheider W and Bichler M 2001 *Nature Phys.* **413** 822

[17] Keyser U F, Fühner C, Borck S, Haug R J, Bichler M, Abstreiter G and Wegscheider W 2003 *Phys. Rev. Lett.* **90** 196601

[18] Liu Y M, Yu Z Y, Jia B Y, Xu Z H, Yao W J, Chen Z H, Lu P F and Han L H 2009 *Chin. Phys.* B **18** 4667

[19] Chi F, Sun L L, Huang L and Zhao J 2011 *Chin. Phys.* B **20** 017303

[20] Jia B Y, Yu Z Y, Liu Y M, Han L H, Yao W J, Feng H and Ye H 2011 *Chin. Phys.* B **20** 067301

[21] Zhai L X, Wang Y and Liu J J 2010 *Phys. Lett.* A **374** 4548

[22] Bercioux D, Governale M, Cataudella V and Ramaglia V M 2004 *Phys. Rev. Lett.* **93** 056802

[23] Bercioux D, Governale M, Cataudella V and Ramaglia V M 2005 *Phys. Rev.* B **72** 075305

[24] Ramaglia V M, Cataudella V, Filippis G D and Perroni C A 2006 *Phys. Rev.* B **73** 155328

[25] Bercioux D, Frustaglia D and Governale M 2005 *Phys. Rev.* B **72** 113310

[26] Koga T, Nitta J and van Veenhuizen M J 2004 *Phys. Rev.* B **70** 161302R

[27] van Veenhuizen M J, Koga T and Nitta J 2006 *Phys. Rev.* B **73** 235315

[28] Koga T, Sekine Y and Nitta J 2006 *Phys. Rev.* B **74** 041302R

[29] Li P and Deng W J 2009 *Acta Phys. Sin.* **58** 2713 (in Chinese)
[30] Szafran B and Poniedzialek M R 2009 *Phys. Rev.* B **80** 155334
[31] Fu B and Deng W J 2010 *Acta Phys. Sin.* **59** 2739 (in Chinese)
[32] Strambini E, Piazza V, Biasiol G, Sorba L and Beltram F 2009 *Phys. Rev.* B **79** 195443
[33] Xia J B 1992 *Phys. Rev.* B **45** 3593
[34] Mireles F and Kirczenow G 2001 *Phys. Rev.* B **64** 024426
[35] Governale M and Zülicke U 2002 *Phys. Rev.* B **66** 073311
[36] Vidal J, Montambaux G and Doucot B 2000 *Phys. Rev.* B **62** R16294
[37] Kottos T and Smilansky U 1999 *Ann. Phys.* (NY) **274** 76
[38] Büttiker M, Imry Y, Landauer R and Pinhas S 1985 *Phys. Rev.* B **31** 6207
[39] Landauer R 1970 *Philos. Mag.* **21** 863
[40] Yi J, Cuniberti G and Porto M 2003 *Eur. Phys. J.* B **33** 221
[41] Lee H W and Kim C S 2001 *Phys. Rev.* B **63** 075306
[42] Kim T S, Cho S Y, Kim C K and Ryu C M 2002 *Phys. Rev.* B **65** 245307